PERGAMON

International Journal of Heat and Mass Transfer 43 (2000) 2529–2539

International Journal of HEAT and MASS TRANSFER

www.elsevier.com/locate/ijhmt

Influence of design parameters on the heat transfer and flow friction characteristics of the heat exchanger with slit fins

Jeom-Yul Yun[a], Kwan-Soo Lee[b,*]

[a]*Home Appliance Research Laboratories, LG Electronics Co., 327-23, Gasan-Dong, Keumchun-Gu, Seoul 153-023, South Korea*
[b]*School of Mechanical Engineering, Hanyang University, Seoul, 133-791, South Korea*

Received 8 July 1999; received in revised form 15 October 1999

Abstract

This study systematically analyzes the effect of various design parameters on the heat transfer and pressure drop characteristics of the heat exchanger with a slit fin. The Taguchi method, known to be a very reasonable tool in a parametric study, is employed in the present work. Only seven cases of experimental factors are considered because of the difficulty in producing samples and the manufacturing cost. Eighteen kinds of scaled-up models are made by compounding levels on each factor, and the heat transfer and flow characteristics of each model are analyzed. The results allow us to quantitatively estimate the various parameters affecting heat exchanger performance, and the main factors for optimum design of a heat exchanger are selected. The optimum design value of each parameter is presented and the reproducibility of the results is discussed.

1. Introduction

Fin-and-tube heat exchangers which have probably been the most widely used heat exchanger for many years have the advantage of reducing the relatively large air-side thermal resistance with the use of interrupted surfaces such as louvers or slits. Air conditioners today are required to be efficient and compact due to regulations on energy consumption. As a result, the development of an enhanced heat exchanger with better performance has been promoted. It is a well known fact that one way to achieve this is to process interrupted surfaces on the fin. These fins have inherent heat transfer characteristics depending upon the shape of the fin, and these characteristics can be more remarkably seen in the slit fin. Hence, it is important to determine the optimum fin shape in the development of a new heat exchanger [1].

Development of heat exchangers through the improvement of fin shapes has been integral to manufacturers. The vigorous effort required to develop a new type of heat exchanger is almost impossible to execute due to the high cost and long development period involved. Previous researchers have focused mainly on the comparative superiority of some idea or the improvement and evaluation of performance through a minor change in design. There has been little work on examining the effect of a design parameter on the interrupted fin itself. The first study on the slit fin and round tube heat exchanger was performed by Nakayama et al. [2]. They reported that the heat exchanger of 2 row, staggered arrangements with the slit fin, which used

* Corresponding author.

0017-9310/00/$ - see front matter
PII: S0017-9310(99)00342-7

Nomenclature

A_o	heat transfer surface area (m^2)
c_p	specific heat at constant pressure (kJ kg^{-1} K^{-1})
D_h	hydraulic diameter, $D_h = 4V_c/A_o$ (m)
f	friction factor, dimensionless
h	heat transfer coefficient (W m^{-2} K^{-1})
JF	JF factor, dimensionless
j	j factor, dimensionless
k	thermal conductivity (W m^{-1} K^{-1})
L	heat exchanger depth in air flow direction (m)
n	degree of freedom
p	pressure (Pa)
P	friction power, $P = q\Delta p$ (W)
Δp	pressure drop (Pa)
P_f	fin pitch (mm)
Pr	Prandtl number, $Pr = c_p\mu/k$
Q	heat transfer rate (W)
r	the number of effective replications
Re	Reynolds number, $Re = \rho V D_h/\mu$
S_m	mean variance for measured data
SN	signal-to-noise
S_T	sum of square for measured data
ΔT_{am}	arithmetic mean temperature difference (K)
T	temperature (K)
v	velocity vector (m s^{-1})
V	air velocity (m s^{-1})
V_c	air-side volume (m^3)
V_e	error sum of squares

Greek symbols

η	signal-to-noise ratio
μ	dynamic viscosity (kg m^{-1} s^{-1})
ρ	air density (kg m^{-3})

Superscript

$*$	nondimensionalization

Subscripts

a	air
f	fin
h	hydraulic
in	inlet, inside tube
m	scaled-up model
p	prototype
R	reference
w	tube wall

9.5 mm tube diameter, 0.2 mm fin thickness and 2 mm slit width, showed a higher heat transfer coefficient by about 78% than that of the plane fin. Due to the design improvement on the various kinds of fin shapes thereafter, they showed better performance better by approximately 150% as compared to the plane fin. A representative case has been proposed by Hiroaki et al. [3]. It has the X-shaped pattern of slits and a 7 mm round tube. They reported accomplishing a 1.6 times heat transfer performance and a two-third compactness over the existing results. In recent years, Koido et al. [4] performed flow visualization tests and numerical analysis using two kinds of slit fins of a 20:1 scaled-up model to investigate the temperature and velocity field, and they determined the shape of the optimum fin.

The existing studies do not explain in detail the optimum design procedure of slits, and hence, the establishment of a reasonable standard for the optimum design is required. In this study, the effects of the various kinds of design parameters on heat transfer and pressure drop characteristics of a heat exchanger with a slit fin are systematically analyzed. The Taguchi method [5–7], known to be a highly reasonable tool in a parametric study, is employed in the present work. The experiments in this study use the scaled-up model as described in our previous work [8]. The results also provide us with quantitative estimation of the various parameters affecting performance, and the main factors for optimum design are selected. The optimum design value of each parameter is presented, and the reproducibility of the results is discussed.

2. Evaluation procedure

2.1. Scaled-up experiment

2.1.1. Theoretical analysis

The nondimensional governing equations of steady, incompressible flows can be written as follows:

$$\nabla^* \cdot v^* = 0 \tag{1}$$

$$(v^* \cdot \nabla^*)v^* = -\nabla^* p^* + \left(1/Re\right)\nabla^{*2} v^* \tag{2}$$

$$(v^* \cdot \nabla^*)T^* = \left(1/Re\,Pr\right)\nabla^{*2} T^* \tag{3}$$

where

$$x^* = \frac{x}{D_h}, v^* = \frac{v}{V}, \nabla^* = D_h\nabla, p^* = \frac{p - p_o}{\rho V^2},$$

$$T^* = \frac{T_w - T}{T_w - T_{in}},$$

$$Re = \frac{\rho V D_h}{\mu}, Pr = \frac{c_p\mu}{k}, D_h = \frac{4V_c}{A_o} \quad (4)$$

The parameters are normalized as Eq. (4). From the above equations, it follows that there exists a similarity between the scaled-up model and the prototype if the Reynolds and Prandtl numbers are the same. Also, a similarity on temperature distribution in the fin has to be maintained for complete similarity. Similitude of fin surface temperature is obtained from the heat conduction equation in the fin as follows:

$$\nabla^* \cdot \left(k_f^* \nabla^* T_f^*\right) = 0 \quad (5)$$

where

$$T_f^* = \frac{T_f - T_{in}}{T_w - T_{in}}, \qquad k_f^* = \frac{k_{f,m}}{k_{f,p}} \quad (6)$$

T_f^* and k_f^* represent dimensionless fin temperature and thermal conductivity, respectively. Since the thermal conductivities of the model and the prototype are the same for the same material, similitude of fin surface temperature may be achieved only if geometric dimensions such as fin thickness are scaled-up with the scale factor.

2.1.2. Experimental apparatus and procedure

Fig. 1 shows the schematic diagram of the experimental apparatus. This apparatus is an open type with a small size wind tunnel. Average air velocity in the test section can be controlled from 0.2 to 1.0 m s^{-1} using a suction fan connected to the power regulator. Static pressure is measured using six pressure taps which are installed at the inlet and outlet of the test section. Pressure drop of the sample is measured by a differential pressure gauge. Average air temperature difference is measured using type T thermocouples installed at the same position. To control the inlet air temperature at the same condition as the real product, an air cooled heat exchanger with a water tank at constant temperature is placed at the inlet section of the chamber. Styrofoam of 40 mm in thickness is used to minimize the heat loss.

The test section is composed of nine sets of fins and one hundred rings equivalent to the tube of the prototype. To maintain wall temperature at the same condition as the actual product, electricity is supplied with nickel–chrome wire inside the ring. Electric power on the first and second rows can be independently controlled with slidacs for the convenience of heat transfer calculation. The amount of heat supplied is measured with a powermeter. The fins and tubes are made of aluminum, and they are fixed by screws to minimize contact resistance. Table 1 shows the comparison of parameters between the two models used in this study.

The experiment starts with controlling the electric power after the fan speed reaches a maximum value. The amount of electric power is measured after the wall temperature reaches a steady state value at every

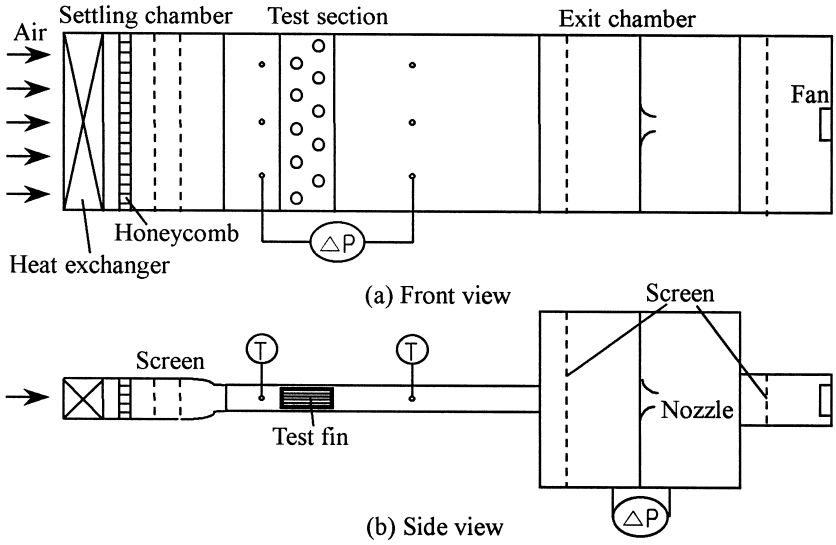

Fig. 1. Schematic diagram of the test apparatus for scaled-up experiment.

measuring point. Steady state is always accomplished after 30 minutes, and the test is repeatedly done with increasing or decreasing air velocity to identify reproducibility. The heat transfer coefficient is obtained as:

$$h = \frac{Q}{A_o \Delta T_{\mathrm{am}}} \tag{7}$$

where Q represents the amount of electric power supplied, and ΔT_{am} indicates the arithmetic mean temperature difference. Colburn j factor and friction factor f, respectively, are given by

$$j = \frac{hPr^{\frac{2}{3}}}{\rho c_p V} \tag{8}$$

$$f = \frac{D_{\mathrm{h}}}{L}\frac{2\Delta p}{\rho V^2} \tag{9}$$

where ρ and c_p represent the air density and the specific heat at constant pressure at the film temperature, respectively.

2.2. Verification of the scaled-up experiment using reference fin

Fig. 2 shows the configurations of a reference fin used in this study. Figs. 3 and 4 show the heat transfer coefficient and pressure drop, respectively, of the scaled-up model and the prototype model with air velocity for this reference fin. The data of the scaled-up model have to be tripled for comparison with those of the prototype model. Hiroaki's result [1,3] on the heat transfer coefficient was obtained by the Wilson plot method [9]. The heat transfer coefficient on the scaled-up model shows relatively good agreement with the prototype results at the air velocity of about 1.0 m s^{-1}, but it is underestimated by 2.7% at the velocity of 1.5 m s^{-1}. Since it seems that the performance estimation on the prototype generally has a measurement error of 3.0%, the present scaled-up model predicts the heat transfer characteristics of the prototype very well. The uncertainty of heat transfer coefficient on the scaled-up experiment is between 3.6% and 4.0% according to the velocity range.

It is shown that pressure drop in the prototype experiment is higher by approximately 3.2% than that of the scaled-up experiment at the velocity of 1.0 m s^{-1}. However, the two results are in good agreement at velocities of over 1.5 m s^{-1}. The uncertainty of pressure drop on the scaled-up experiment is 2.8% to 5.0% according to the velocity range. Since pressure drop of a resistance body is proportional to the square of the velocity, the scaled-up experiment results fitted to a quadratic curve can be closer to the actual state as compared to the prototype results. Hence, a scaled-up model can also predict the heat transfer coefficient and the pressure drop more accurately. These results can effectively be used in the development of a new heat exchanger.

2.3. Selection of characteristics

Since, in general, an increase in heat transfer yields an increase in pressure drop, one must consider the trade-off between the increased heat transfer and the increased pressure drop in evaluating the performance of a heat exchanger. However, as it is difficult to simultaneously evaluate both the heat transfer coefficient of larger-the-better and the pressure drop of smaller-the-better, an evaluation characteristics value considering these two effects simultaneously should be demanded to perform an effective parametric study on a heat exchanger with a slit fin using the Taguchi method.

It is a well known fact that j and f factors are the relevant parameters used to characterize the heat transfer coefficient and the pressure drop, respectively, of a

Table 1
Comparison of similitude relations on physical parameters in this study

Physical parameters	Scaled-up model	Prototype model
Scale factor	3	1
Fin length (mm)	3	1
Fin thermal conductivity (W m^{-1} K^{-1})	1	1
Fin thickness (mm)	3	1
Fin surface temperature (K)	$T(x, y)$	$T(x, y)$
Air velocity (m s^{-1})	1/3	1
Heat transfer rate (W)	3	1
Heat transfer coefficient (W m^{-2} K^{-1})	1/3	1
Pressure drop (Pa)	1/9	1
Re, Pr number	1	1
j, f factor	1	1

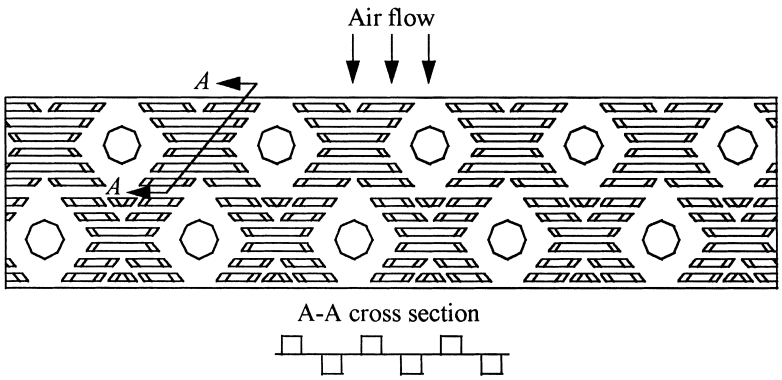

Fig. 2. Configuration of reference fin.

heat exchanger. But, a direct comparison on the basis of j and f factors, in evaluating the performance of a heat exchanger, is not useful in selecting the optimum one, because if j is large, f also becomes large. Thus, we need a relevant nondimensionalized parameter to simultaneously define the heat transfer and flow friction characteristics according to fin shapes between the comparative heat exchangers. This is derived from the performance evaluation criteria based on area goodness factor which has been proposed to compare the thermal and dynamic performance of heat exchangers. This can be obtained using the two ratios between a heat exchanger tested and a reference heat exchanger; one for heat transfer rate (h) per unit temperature difference, per unit surface area, and the other for friction power (P/A) dissipated per unit surface area. The heat transfer performance h and the friction power P/A are respectively expressed by a function of j, f and Re/D_h as follows [1,10]:

$$h = \left(\frac{\rho c_p}{Pr^{2/3}}\right) jV = \left(\frac{\mu c_p}{Pr^{2/3}}\right) j\left(\frac{Re}{D_h}\right) \tag{10}$$

$$\frac{P}{A} = \left(\frac{\rho}{2}\right) fV^3 = \left(\frac{\mu^3}{2\rho^2}\right) f\left(\frac{Re}{D_h}\right)^3 \tag{11}$$

Dividing Eqs. (10) and (11) by the corresponding parameters of the reference heat exchanger, respectively, gives

$$\frac{h}{h_R} = \frac{j(Re/D_h)}{j_R(Re/D_h)_R}, \qquad \frac{P/A}{(P/A)_R} = \frac{f(Re/D_h)^3}{f_R(Re/D_h)_R^3} \tag{12}$$

Combining the two equations of Eq. (12) gives

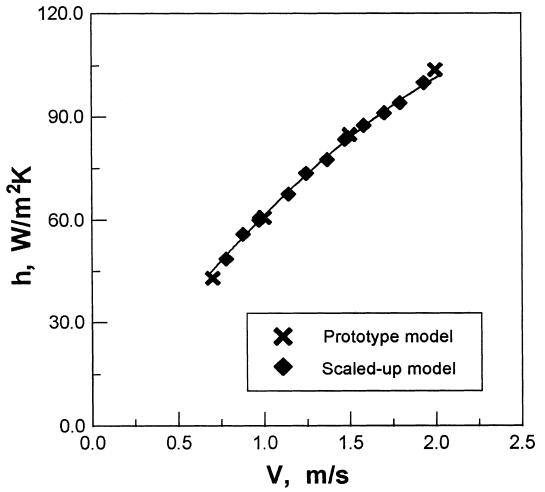

Fig. 3. Comparison of the heat transfer coefficients for scaled-up and prototype models using reference fin.

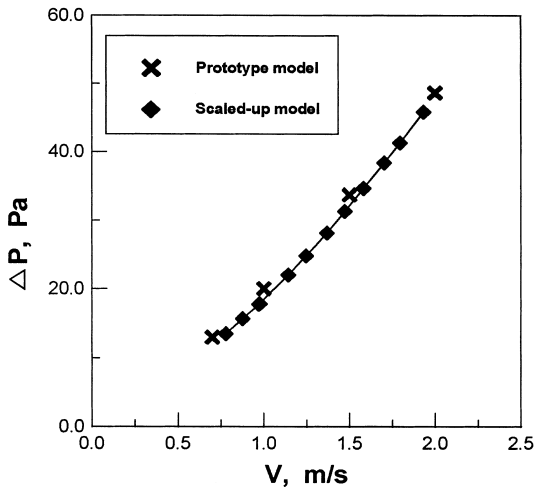

Fig. 4. Comparison of the pressure drop for scaled-up and prototype models using reference fin.

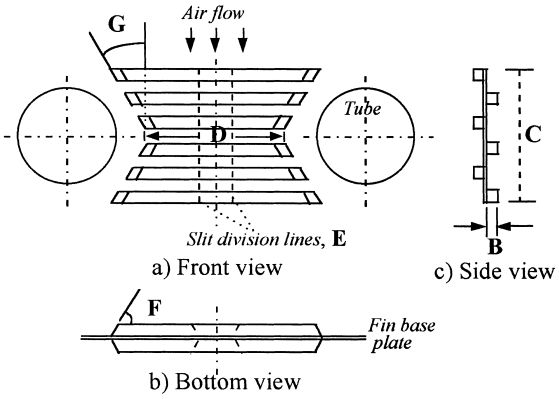

B : Slit height, C : The number of slit, D : Slit length,
E : The number of slit division, F : Raised angle of slit, G : Angle of slit pattern

Fig. 5. A detail of control factors in this study.

$$\frac{h/h_R}{\left\{(P/A)/((P/A)_R)\right\}^{1/3}} = \frac{j/j_R}{(f/f_R)^{1/3}} \tag{13}$$

Finally, the term on the right-hand side of Eq. (13) which considers j and f factors simultaneously is newly named the JF factor in the present study:

$$JF = \frac{j/j_R}{(f/f_R)^{1/3}} \tag{14}$$

This is a dimensionless number of larger-the-better characteristics. As can be seen from Eq. (14), it is expected that this parameter can effectively evaluate the thermal and dynamic performance of a heat exchanger since it includes both the j and the f factor. The j and f factors on the reference heat exchanger use the experimental results for the fin shapes shown in Fig. 2.

2.4. Factors and level

The control factors used in this study are made up of seven factors related to the heat transfer surface area and the turbulence in the air-side. A detailed explanation of these factors is presented in Fig. 5. The levels are based on the currently used dimensions of the coil with a 7 mm tube diameter, and these are selected considering the present manufacturing technology. As shown in Table 2, interaction with the FPI is excluded by selecting one-third, a half and two-thirds of the fin pitch, as far as the slit height is concerned. The C, D, E terms of two levels are changed to three levels by using the dummy level technique, and the angle of slit pattern, G, of four levels is coordinated with six levels by the same method. In order to change two levels of a factor into three levels, the most important (standard) level must be duplicated in the experimental matrix. The method of duplicating a level is called the dummy level technique. The air velocity is

Table 2
Levels of each factor in this study

Code	Factors (unit)	Level 1	Level 2	Level 3
A	Fin pitch, P_f (mm)	1.49	1.34	1.2
B	Slit height (mm)	1/3 P_f	1/2 P_f	2/3 P_f
C	The number of slits	6	8	6
D	Slit length (mm)	10	8	10
E	The number of slit divisions	1	2	1
F	Raised angle of slit (°)	45	35	25
G	Angle of slit pattern (°) (inlet angle/outlet angle)	0/0	0/30	30/0
		30/30	0/0	30/30

taken as the signal factor, and the noise factor is not considered in this study. Fin thickness, step pitch and row pitch are considered as the fixed factor.

2.5. Experimental matrix

The experimental matrix uses the orthogonal array of L_{18} which is based on the geometric factor in this study, as shown in Table 3. This is an array of $L_{18}(6^1 \times 3^6)$ which is modified from the array of $L_{18}(2^1 \times 3^7)$. The signal factor is applied to only eleven measuring points.

2.6. Experimental model

Fig. 6 represents the basic geometry of a 3:1 scaled-up model fin. The experimental samples are used to manufacture the various shapes of slits on the fin surface by coordinating the levels as shown in Table 2. These are made by a fin die in order to make them more accurate, and the fin material is aluminum. Eighteen kinds of samples are made by a combination of levels on the orthogonal array as indicated in Table 3.

2.7. Analysis

The signal-to-noise ratio used in the analysis of the Taguchi method is a measure that is particularly useful

Table 3
The orthogonal array of $L_{18}(6^1 \times 3^6)$

Number of test	Control factor							Signal factor V_i (air velocity)
	G	A	B	C	D	E	F	
	1	2	3	4	5	6	7	
TS1	1	1	1	1	1	1	1	
TS2	1	2	2	2	2	2	2	
TS3	1	3	3	3	3	3	3	
TS4	2	1	1	2	2	3	3	
TS5	2	2	2	3	3	1	1	
TS6	2	3	3	1	1	2	2	
TS7	3	1	2	1	3	2	3	
TS8	3	2	3	2	1	3	1	
TS9	3	3	1	3	2	1	2	
TS10	4	1	3	3	2	2	1	
TS11	4	2	1	1	3	3	2	
TS12	4	3	2	2	1	1	3	
TS13	5	1	2	3	1	3	2	
TS14	5	2	3	1	2	1	3	
TS15	5	3	1	2	3	2	1	
TS16	6	1	3	2	3	1	2	
TS17	6	2	1	3	1	2	3	
TS18	6	3	2	1	2	3	1	

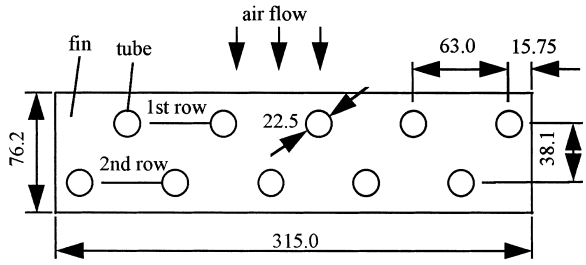

Fig. 6. Basic geometry of a 3:1 scaled-up model fin, all dimensions in mm.

for process design. The objective performance should not vary much with large changes in the environment or in raw materials in the actual machine. In order to select the levels of control factors more efficiently, we can transform our data into the SN ratio. A larger SN ratio is preferred. This SN ratio is calculated from the data of the worst condition and the standard condition for each experiment given by an orthogonal array. The SN ratio in this study is defined by the following equation representing the dynamic characteristics [6]:

$$SN(=\eta) = 10\log\left(\frac{1}{r} \times \frac{(S_m - V_e)}{V_e}\right) \tag{15}$$

where

$$r = \sum_{i=1}^{n} V_i^2, \qquad S_m = \frac{\left(\sum_{i=1}^{n}(V_i \times JF_i)\right)^2}{r}, \tag{16}$$

$$V_e = \frac{S_e}{n-1}, \qquad S_e = S_T - S_m, \qquad S_T = \sum_{i=1}^{n} JF_i^2$$

Here, V_i and JF_i represent the ith air velocity and the ith JF factor, respectively. These data are taken at eleven points for air velocity as mentioned before.

3. Results and discussion

3.1. Factorial effect and contribution ratio

Table 4 shows the SN ratios calculated from the eighteen tests. The factorial effect and contribution ratio of each factor from those ratios are presented in Table 5 and Fig. 7. The SN ratios of levels on each factor in Table 5 are calculated from the arithmetic average of SN ratios corresponding to each level given in Table 4. The contribution ratio means the effect of each factor on the JF factor, namely, the performance characteristics of a heat exchanger. This is calculated using R that indicates the difference between maximum

Table 4
SN ratio on each experiment

Number of test	Control factor							SN ratio (η)
	G 1	A 2	B 3	C 4	D 5	E 6	F 7	
TS1	1	1	1	1	1	1	1	17.13799
TS2	1	2	2	2	2	2	2	17.27338
TS3	1	3	3	3	3	3	3	18.34859
TS4	2	1	1	2	2	3	3	16.72726
TS5	2	2	2	3	3	1	1	17.98196
TS6	2	3	3	1	1	2	2	18.63592
TS7	3	1	2	1	3	2	3	17.21723
TS8	3	2	3	2	1	3	1	17.55372
TS9	3	3	1	3	2	1	2	17.30539
TS10	4	1	3	3	2	2	1	17.23327
TS11	4	2	1	1	3	3	2	18.39126
TS12	4	3	2	2	1	1	3	18.63518
TS13	5	1	2	3	1	3	2	16.78063
TS14	5	2	3	1	2	1	3	17.20862
TS15	5	3	1	2	3	2	1	17.92852
TS16	6	1	3	2	3	1	2	17.94397
TS17	6	2	1	3	1	2	3	17.99606
TS18	6	3	2	1	2	3	1	18.35967

and minimum of the SN ratio on each factor. As a result, the contribution ratio of each factor is obtained from the ratio of R corresponding to each factor to total R. Thus, the effect of each factor on the *JF* factor of the slit fin is enumerated as 39% for fin pitch, 28% for angle of slit pattern, 20% for slit length, 9% for slit height among seven factors as presented in Table 5 and Fig. 7. The other factors have a trifling effect on the *JF* factor. Therefore, it is clear that the contribution ratio of the factors such as the number of slits, the number of slit divisions and the raised angle of the slit is lower by 2%, however, the factors such as the slit length, the angle of slit pattern, the slit height and the fin pitch have greatly influenced the *JF* factor of a heat exchanger. The contribution ratio of the fin pitch is the largest among the factors considered, and the contribution of the other ratios are shown in the order of the angle of slit pattern, the slit length, the slit height, and so on. However, note that the present results on the contribution ratio is limited to the effects of the seven factors used in this study. Hence, to investigate the effects of factors other than those above, one can repeat a similar procedure.

Fig. 8 shows the SN ratio of each factor to be considered in selecting the optimum condition. It means that the largest SN ratio level of all the levels on each factor has the best performance as mentioned above. As far as the fin pitch is concerned, 3.6 mm is the best. Since the angle of slit pattern of 30°/30° in the inlet/outlet shows the largest SN ratio among all the levels, it is clear that the *JF* factor has the maximum effect by forming as many slits as possible within the maximum allowable area. The formation of 30°/0° is distinctly lower when compared to that of 0°/30°. It is confirmed from these facts that the slits should be designed to minimize the dead zone in the rear flow. The slit height is the best in the case of two-thirds of a fin pitch. The number of slits has the optimum condition at the 6 array group. Therefore, it is not good to recklessly increase the number of slits for the purpose of maximizing the leading edge effect. The slit length at the central section indicates the optimum condition at the 10 mm level. Although it is clear that a longer slit has better performance, it depends on the manufacturing technology. As far as the number of slit divisions is concerned, it is applied to the most common method that has a section to decrease the number of cases in this study. The case of the 2 slit division shows a larger SN ratio than that of the one without division, but there is only a small difference between the two levels. The raised angle of slit has the optimum value at 35°, but it does not greatly influence overall performance.

As shown above, it is confirmed that the factors related to the forming area of the slits and the turbulence of flow are very important parameters in the design of the heat exchanger with the slit fin.

Table 5
Factorial effect and contribution ratio

	Level	Control factor						
		G	A	B	C	D	E	F
SN ratio (η)	1	17.44629	17.17339	17.58108	17.71638	17.87925	17.69785	17.69919
	2	17.78171	17.73417	17.70801	17.67701	17.35127	17.71406	17.72176
	3	17.35878	18.20221	17.82068				17.68882
	4	18.09324						
$R(\eta_{max} - \eta_{min})$	2.619	0.73446	1.02882	0.2396	0.03937	0.52798	0.01621	0.03294
Contribution ratio (%)	100	28.04	39.28	9.15	1.50	20.16	0.62	1.25

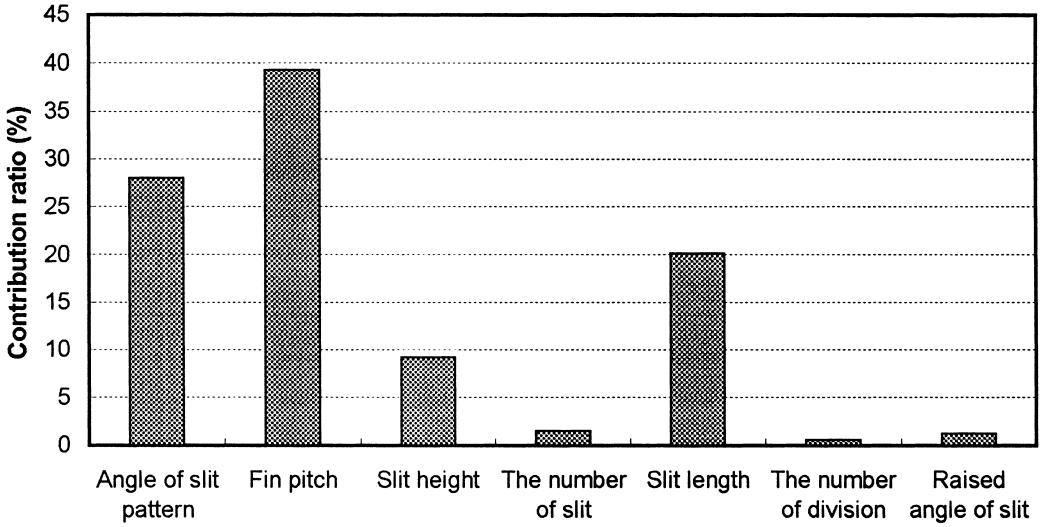

Fig. 7. Contribution ratio on each factor.

3.2. Determination of the optimum condition

The optimum condition is obtained by a combination of levels showing the largest SN ratio in each control factor as presented in Table 5. As a result, two optimum conditions are especially selected in this work as shown in Table 6. Actually, only one optimum condition can be obtained using the present method, but a second best optimum condition is considered in this study, since the E factor has the smallest contribution ratio among all the factors as shown in Table 5. Thus, one original optimum condition (optimum condition 2) is determined based on the Taguchi analysis method, and a second best optimum condition (optimum condition 1) is selected to eliminate the error of analysis due to the small difference in the SN ratio between two levels among all the factors, namely the SN ratio of the number of slit divisions. These two optimum conditions are $G_4A_3B_3C_1D_1E_2F_2$ and $G_4A_3B_3C_1D_1E_1F_2$, respectively.

3.3. Reproducibility by confirmation test

The two test samples are designed by combining the seven factors which are selected to be the optimum conditions as described above, and we have performed the confirmation test using these two samples. This is to confirm the reproducibility of the obtained results. These are divided into three methods.

The first method judges the degree of agreement between the presumed SN ratio for the optimum condition and the SN ratio of confirmation test results for the optimum samples. The presumed SN ratio, η_{pre}, is

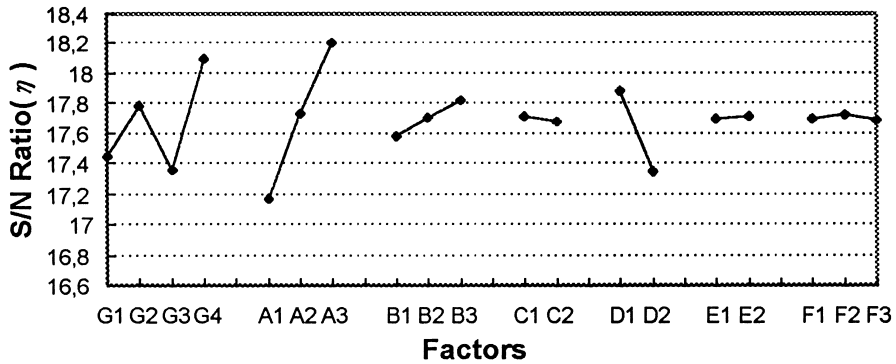

Fig. 8. SN ratio on each factor.

Table 6
Optimum conditions from factorial effect analysis[a]

	Angle of pattern (°)	Fin pitch (mm)	Slit height (mm)	The number of slits	Slit length (mm)	The number of slit division	Raised angle of slit (°)
Optimum condition 1	30/30	3.6 (1.2)	$2/3P_f$ (0.8)	6	30 (10)	1	35
Optimum condition 2	30/30	3.6 (1.2)	$2/3P_f$ (0.8)	6	30 (10)	2	35

[a] Values in parentheses are dimensions of prototype model.

calculated using the factors with a contribution ratio of more than 10% among all factors as follows [6,7]:

$$\begin{aligned}\eta_{pre} &= \eta_{G4} + \eta_{A3} + \eta_{D1} - (m-1)\bar{\eta} \\ &= 18.0932 + 18.2022 + 17.8793 - (3-1) \\ &\quad \times 17.6866 \\ &= 18.8015 \end{aligned} \tag{17}$$

Here, the numerical values of η_{G4}, η_{A3} and η_{D1} are taken from Table 5 and m indicates the number of attentive factors. The SN ratio of the optimum condition 2 obtained directly from the confirmation test was 18.4152. Thus, it is confirmed that there is a reproducibility in this condition, since this value is in good agreement, within 2%, with the presumed value from Eq. (17).

The second method is to compare directly the heat transfer coefficient and the pressure drop of the two optimum conditions. Figs. 9 and 10 represent, respectively, the heat transfer coefficient and pressure drop of the reference sample as shown in Fig. 2 and the two kinds of optimum samples. The heat transfer coefficient of optimum condition 1 is higher by 1.9% than that of optimum condition 2 over the whole test range. This is due to the fact that the turbulence effect is more vivid by the slits at the central section of optimum condition 1. The heat transfer coefficient of optimum condition 1 is lower by about 2.5% than that of the reference fin, known to have the best performance among the existing fins over the whole test range; and that of optimum condition 2 is lower by about 3.4% than that of the reference fin. These show approximately the same performance as the reference fin formed with the complicated patterns. The pressure drop of optimum condition 1 is lower by about 20.5% than that of the reference fin over the whole test range, and that of optimum condition 2 is lower by about 24.7% than that of the reference fin. Hence, it is highly probable to design a fin with a relatively lower pressure drop under the same heat transfer coefficient. The

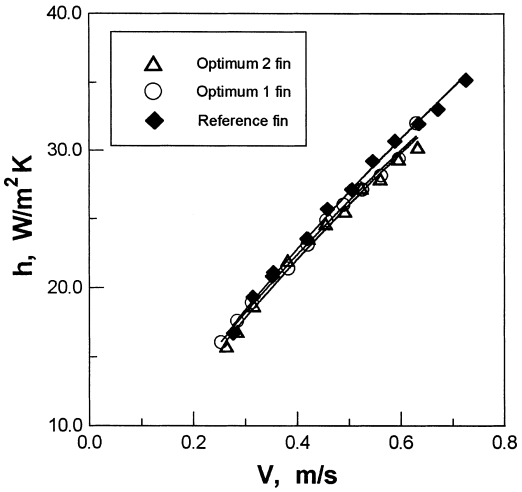

Fig. 9. Comparison of heat transfer coefficients between optimum fins and reference fin.

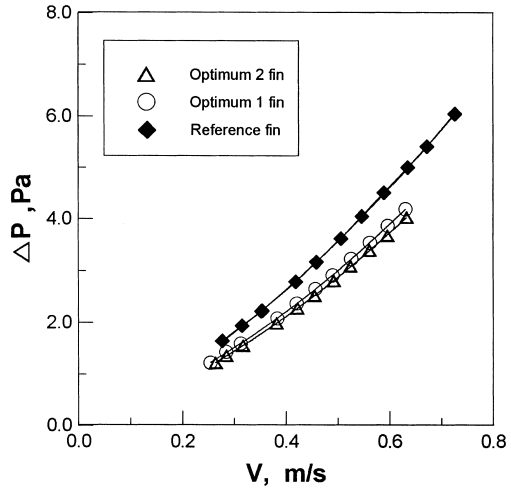

Fig. 10. Comparison of pressure drop between optimum and reference fins.

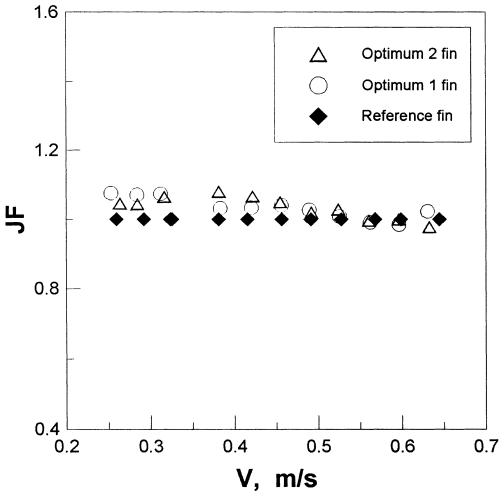

Fig. 11. *JF* factor of optimum fins compared to reference fin.

reproducibility is also verified by the direct comparison above. Since the pressure drop of optimum condition 1 is higher by about 4.2% than that of optimum condition 2 over the whole test range, it is believed that one slit division like this has a small effect on the pressure drop. As a result, when considering the heat transfer and the pressure drop characteristics simultaneously, the optimum fins are superior to the reference fin.

The last method is to confirm the reproducibility by direct comparison of the *JF* factor. Fig. 11 shows the *JF* factor of the optimum fins with air velocity, where that of the reference fin is close to unity. The *JF* factor of the optimum fins is considerably higher than that of the reference fin below the velocity of 0.55 m s^{-1}, which is equivalent to 1.65 m s^{-1} in the prototype. It is thus demonstrated that they perform better at the operating ranges of actual home air conditioners, therefore, reproducibility is verified by the above three cases.

4. Conclusions

In this study, the effects of the various kinds of design parameters on heat transfer and flow characteristics of the heat exchanger with slit fins were systematically analyzed using the Taguchi method. Our conclusions from this study are as follows:

1. The order of magnitude of the effects of each factor on the performance of the heat exchanger with slit fins are as follows: fin pitch (39%), angle of slit pattern (28%), slit length (20%), slit height (9%) among the seven factors presented in this study. The other factors have a contribution ratio of about 1%. The factors related to the slit forming area, especially, have a higher influence on the performance of the heat exchanger.
2. The optimum conditions of each factor are determined, and the reproducibility of these conditions has been verified by three analytical results. It is noted that these show superior characteristics compared to a reference fin.
3. It is shown that the *JF* factor could be a proper tool in the parametric study of a heat exchanger and can be used for the development of a fin with better performance.

Acknowledgements

One of the authors (Dr. Kwan-Soo Lee) wishes to acknowledge the financial support of the Center for Innovative Design Optimization Technology (iDOT), Korea Science and Engineering Foundation (KOSEF).

References

[1] P. Baggio, E. Fornasieri, Air-side heat transfer and flow friction: theoretical aspects in recent development in finned tube heat exchanger, in: Ch. Marvillet (Ed.), DTI, Energy Technology, Denmark, 1994, pp. 91–159.
[2] W. Nakayama, L.P. Xu, Enhanced fins for air-cooled heat exchanger-heat transfer and friction factor correlations, Proc. of the 1983 ASME-JSME Thermal Eng. Conf. 1 (1983) 495–502.
[3] K. Hiroaki, I. Shinichi, A. Osamu, K. Osao, High efficiency heat exchanger, National Technical Report 35 (1989) 71–79.
[4] T. Koido, et al., Development of compact heat exchanger for air conditioner, in: Proceedings of the 26th JAR Annual Conference, 1992, pp. 165–168.
[5] G. Taguchi, Taguchi on robust technology development, Bring Quality Engineering (QE) Upstream ASME, 1991.
[6] T. Mori The New Experimental Design: Taguchi's Approach to Quality Engineering, ASI Press, 1990.
[7] G. Taguchi, A.E. Elsayed, C.H. Thomas, Quality Engineering in Production Systems, McGraw-Hill, New York, 1989.
[8] J.Y. Yun, K.S. Lee, Investigation of heat transfer characteristics on various kinds of fin-and-tube heat exchangers with interrupted surfaces, Int. J. of Heat and Mass Transfer 42 (13) (1999) 2375–2385.
[9] H.F. Khartabil, R.N. Christensen, D.E. Richards, A modified Wilson plot technique for determining heat transfer correlations, in: 2nd U.K. National Conference on Heat Transfer, September, 1989.
[10] R.L. Webb, Principles of Enhanced Heat Transfer, Wiley, New York, 1994 (Chapter 3).